

1 **Encrusting bryozoan attached to terrestrial plant leaves from**
 2 **brackish deposits of the Lefipán Formation (Patagonia, Argentina),**
 3 **close to the K/Pg boundary.**

4 Taboada, César Augusto^{1,*}; Pagani, María Alejandra¹; Cúneo, Rubén¹

5 ¹ Consejo Nacional de Investigaciones Científicas y Técnicas (CONICET) - Museo

6 Paleontológico Egidio Feruglio (MEF), Av. Fontana 140, Trelew, Chubut Province, Argentina.

7 *Corresponding author <ctaboada@mef.org.ar>

8 **Abstract.**—Cretaceous bryozoans from South America have received limited attention despite
 9 their sporadic documentation. The K/Pg boundary has been identified in numerous fossil-rich
 10 basins in Patagonia, where bryozoans are frequent components of the faunas. Material recovered
 11 from upper Maastrichtian outcrops of the Lefipán Formation in the Cañadón Asfalto Basin
 12 (Patagonia, Argentina) includes a unique species of cheilostome bryozoan, *Conopeum foliorum* n.
 13 sp., attached to leaf remains of terrestrial plants and associated with scarce euryhaline bivalves. It
 14 likely thrived in a warm climate, shallow, well-lit brackish environment influenced by tides,
 15 located along the northwest margin of the Paso del Sapo embayment. *Conopeum foliorum* n. sp.
 16 is currently among the earliest known bryozoans from brackish water environments, and the
 17 second oldest documented instance of a bryozoan encrusting leaves of terrestrial plants,
 18 representing the first of such finding in South America. Based on our findings and available
 19 sedimentological and paleoecological data from previous studies, we interpreted *Conopeum*
 20 *foliorum* n. sp. as a fast-growing opportunistic taxon displaying euryhaline habits and prone to
 21 colonize terrestrial plant leaves deposited in a brackish-water nearshore environment.

22 **Keywords:**

23 Taxonomy

24 Bryozoa
25 Maastrichtian
26 Cañadón Asfalto Basin
27 South America
28

29 **1. Introduction**

30

31 The Cretaceous/Paleogene (K/Pg) boundary represents one of the most significant extinction
32 events globally, impacting the biota worldwide. In South America, this boundary is well
33 documented in several highly fossiliferous Patagonian basins in which bryozoans are also found.
34 Studies of these basins have revealed significant differences in the impact of the extinction event
35 between the northern and southern hemispheres. For instance, research has shown lower
36 extinction rates across the boundary followed by a rapid recovery in the Danian period for
37 palynomorphs, plant-insect associations, and marine benthic molluscs (Barreda et al., 2012;
38 Aberhan and Kiessling, 2014; Donovan et al., 2016, 2018). Interestingly, bryozoan diversity in
39 Patagonia exhibits little change across the K/Pg boundary, resembling patterns observed in the
40 northern hemisphere (i.e., Europe, United States) (Brezina et al., 2021).

41 Bryozoans are exclusively aquatic, colonial suspension-feeding benthic animals with a
42 worldwide distribution despite their predominantly sessile mode of life, including some
43 cosmopolitan genera. Upper Cretaceous (Campanian/Maastrichtian) bryozoans are predominantly
44 found in mid-latitudes between 30-60° in both hemispheres, associated with warm-temperate
45 climatic belts (Di Martino and Taylor, 2013); however, they have also been identified in tropical

46 settings from the Tethys, without significant taxonomic differentiation from those at higher
47 latitudes (Di Martino and Taylor, 2013; Taylor, 1995). Cretaceous bryozoans have primarily been
48 documented in Europe, North America, Central Asia, Madagascar, India, and Australia, while
49 records from South America are limited (among others Taylor, 2019; Brezina et al., 2021; Taylor
50 and Roger, 2021; Sonar et al., 2023; Håkansson et al., 2024; and references therein). In
51 Argentina, Cretaceous bryozoan records are restricted to the Neuquén Basin in northern
52 Patagonia (Canu, 1911; Taylor et al., 2009; Brezina et al., 2021).

53 Herein we report new records of Cretaceous bryozoans encrusting leaves of terrestrial plants,
54 briefly discussed previously by the present authors (Taboada et al., 2018). We provide a detailed
55 taxonomic analysis of the bryozoans and interpretations of their paleoecological significance.
56 Finally, we propose a new species of bryozoan, being the first to be formally described from the
57 Cañadón Asfalto Basin in central Patagonia.

58

59 **2. Geological settings**

60 The studied specimens were collected from the Lefipán Formation which overlies
61 conspicuous outcrops of the Paso del Sapo Formation; these units characterize the final infilling
62 of the Cañadón Asfalto Basin, Chubut Province, Patagonia, Argentina (Figure 1A, B). The
63 Lefipán Formation is a siliciclastic unit with continuous intercalated sandstones and mudstones
64 with some coquinas and conglomerates (Medina and Olivero, 1994). The age of the Lefipán
65 Formation is constrained by biostratigraphic proxies to be Maastrichtian/Danian (Barreda et al.,
66 2012). The Lefipán Formation has been interpreted as grading from estuarine or tide-dominated
67 deltaic conditions in the Maastrichtian to a more open marine environment in the Danian, as part

68 of a shallow embayment (named as Paso del Sapo embayment by Scasso et al., 2012) in the
 69 southern branch of the Kawas Sea (Casamiquela, 1978; Goin et al., 2016). This setting
 70 corresponds approximately to a paleolatitude of 45 to 48°S in a warm-temperate climatic belt
 71 (Olivero and Medina, 1994; Scotese, 2004; Nañez and Malumián, 2008; Cúneo et al., 2021;
 72 Scasso et al., 2012).

73 One of the best exposures of the Lefipán Formation corresponds to the San Ramón
 74 Section (Figures 1C, 2), located 20 km W of Paso del Sapo village and 3 km south of the Chubut
 75 River. This stratigraphic section is approximately 400 m thick, 270 m of which are of
 76 Maastrichtian age (Scasso et al., 2012). The studied bryozoans were collected from a single
 77 fossil-bearing bed indicated as PLE –after *Perfil Lefipán* East– on the figured section (= LefE as
 78 detailed in Donovan, et al., 2016, 2018; Wilf et al., 2017; Escapa et al., 2018; Stiles et al., 2020)
 79 (Figure 1C). The stratigraphic position of the PLE lies within the terminal Maastrichtian,
 80 presumably a few stratigraphic meters above the monotypic *Corbicula* assemblage and 21.5 m
 81 below the lower Paleocene (lower Danian) *Turritella* marker bed as described in Scasso et al.,
 82 (2012) (Figure 1C).

83 Five facies associations and eight biofacies were recognized from the Lefipán Formation
 84 by Scasso et al. (2012). PLE belongs to lithofacies H2 (weakly bioturbated heterolithics), and
 85 consists of horizontally laminated mud-sand couplets with coaly plant remains in the muddy part.
 86 Sedimentary environments for H2 correspond to tidal flats near vegetated coasts (marsh) along
 87 the margins of tide-dominated delta channels with substantial salinity reduction at the K/Pg
 88 boundary, changing to oxygenated subtidal transitional environments with rapid sedimentation
 89 and frequent changes in salinity in the Danian (Scasso et al., 2012). In this sense, sand deposition
 90 occurred during periods of current activity and mud deposition during tidal slack-water periods

91 (Scasso et al., 2012). Further, H2 is often found around the K/Pg boundary within upper levels of
 92 Facies Association III (tidal channel, tidal gully and tidal flat deposits) at the San Ramón Section
 93 (Scasso et al., 2012). The following biofacies have been associated, but not necessarily restricted
 94 to the lithofacies H2: *Struthioptera-Panopea* association in the Maastrichtian, *Corbicula* faunal
 95 assemblage at the K/Pg boundary, and *Corbicula-Venericardia* followed by *Meretrix-Ledina*
 96 associations in the early Danian (Scasso et al., 2012). The former authors did not record
 97 bryozoans associated with the lithofacies, biofacies mentioned above or with any other fossil-
 98 bearing bed from the Lefipán Formation.

99

100 **3. Material and methods**101 *3.1. Material preservation and preparation*

102 Bryozoans appear as adjacent and nearly neighbouring colonies encrusting plant leaves.
 103 They are regularly preserved in two ways: attached to plant leaves with exposed frontal surfaces
 104 or as natural moulds produced by sediment infilling. In the first case, morphological
 105 characteristics are poorly preserved. In the second, a silicon rubber cast was prepared for one
 106 sample following Kelly and McLachlan (1980). Similar preservation was described in Dick et al.
 107 (2009). Samples were cleared of sediment with a hand brush, and some were coated with
 108 sublimated magnesium oxide for the first optical microscopy exploration (Jeffords and Miller,
 109 1960).

110

111 *3.2. Morphological data collection*

112 Linear measurements were obtained on digital images using Image J software (Schneider
113 et al., 2012; <https://imagej.net>). Coated specimens were photographed optically with digital
114 cameras at the Museo Paleontológico Egidio Feruglio (MEF). Some details were also
115 photographed from uncoated specimens with a Jeol JSM-6460LV scanning electron microscope
116 (SEM) in low vacuum and backscattered electron signal conditions (at ALUAR S.A., Puerto
117 Madryn, Chubut). Because of the low relief of the colonies they are challenging to photograph.
118 All morphological measurements are in millimetres, and they are presented as arithmetic mean
119 (Mean), sample standard deviation (SD), coefficient of variation (CV), minimum and maximum
120 values (MIN and MAX respectively), and number of measurements made (N). Measurement
121 abbreviations: autozooid length as seen on colony surface (ZL); autozooid width as seen on
122 colony surface (ZW).

123

124 *3.3. Repository and institutional abbreviation*

125 Studied specimens are stored under the prefix MPEF-PI at the MEF's paleo invertebrate
126 collection in Trelew, Chubut, Argentina.

127

128 **4. Systematic paleontology**

129

130 Phylum **Bryozoa** Ehrenberg, 1831

131 Classs **Gymnolaemata** Allman, 1856

132 Order **Cheilostomata** Busk, 1852

133 Suborder **Membraniporina** Ortmann, 1890

134 Superfamily **Membraniporoidea** Busk, 1852

135 Family **Electridae** Stach, 1937

136 Genus ***Conopeum*** Gray, 1848

137 *Type species.* *Millepora reticulum* Linnaeus, 1767, Recent, North Atlantic Ocean.

138

139 *Occurrence.* Worldwide. Upper Cretaceous to Recent.

140

141 *Remarks.* Based on features observed, our specimens are assigned to *Conopeum*. Key diagnostic

142 features of *Conopeum* include the presence of a single, non-twinned ancestrula; development of

143 normally unilaminar, multiserial encrusting colonies; elongate autozooids with extensive opesia;

144 gymnocyst absent or poorly developed relative to the cryptocyst; and absence of ovicells and

145 avicularia (after Hayward and Ryland, 1998; Dick et al., 2014; Gordon et al., 2020; Taylor and

146 Rogers, 2021). Our specimens align closely with the defining traits of *Conopeum*.

147 *Conopeum* differs from the two Maastrichtian *Conopeum*-like genera *Eokotosokum*

148 Taylor and Cuffey, 1992 and *Bullaconopeum* Taylor, 1995 in the absence of two large

149 distolateral spine bases and four prominent gymnocystal tubercles, respectively (see Taylor and

150 McKinney, 2006). The Albian/Maastrichtian genus *Iyarispora* Martha, Taylor and Rader, 2019

151 differs from *Conopeum* mainly in having some zooids with calcified closure plates containing

152 pores (Martha et al., 2019; Taylor and Rogers, 2021). The Cenomanian/Maastrichtian genus

153 *Heteroconopeum* Voigt, 1983 differs from *Conopeum* in having erect colonies comprising

154 narrow, transversally cylindrical branches with distinct endozone and exozone (Voigt, 1983;

155 Taylor and Rogers, 2021).

156 Therefore, based on these comparative morphological characteristics, *Conopeum* remains
 157 the most suitable genus for the taxonomic assignment of our specimens.

158

159 *Conopeum foliorum* new species

160 Figures 3–5; Table 1

161 *LSID identifier.* urn:lsid:zoobank.org:act:6D236CA5-2EBE-4630-A800-C24B6F0FFB2A

162

163 *Derivation of name.* In reference to its occurrence attached to leaves of diverse terrestrial plants,
 164 *foliorum* (Latín) of the leaves.

165

166 *Material.* Holotype: MPEF-PI 7101-1; paratypes: MPEF-PI 7101-2; MPEF-PI 7101-3; MPEF_PI
 167 7102-1; MPEF_PI 7102-2; MPEF_PI 7102-3; MPEF_PI 7106 (a-b). Additional material:
 168 MPEF_PI 7103 (a-b); MPEF_PI 7104 (a-b); MPEF_PI 7105 (a-b); MPEF_PI 7107 (a-b). From
 169 the PLE heterolithic fossil-bearing bed located 20 km west of Paso del Sapo village and 3 km
 170 south of the Chubut River, 21.5 m stratigraphically below the K/Pg boundary at the San Ramón
 171 section, Lefipán Formation (Cañadón Asfalto Basin).

172

173 *Diagnosis.* Colony unilaminar, spot- to sheet-like. Ancestrula budding a distal and two
 174 distolateral zooids. Autozooids medium-sized, elongate rectangular with extensive opesia,
 175 arranged in a brickwall-like alternation pattern between adjacent rows; gymnocyst absent;
 176 cryptocyst narrow forming a thin mural rim, with rarely preserved rounded granules; spine bases
 177 and closure plates not observed, presumably absent. Kenozooids not observed.

178

179 *Description.* Colony encrusting, unilaminar and multiserial, with radial growth pattern (Figures
 180 3A-B; 4A-B; 5A). Early astogeny is commonly preserved. The ancestrula is single, oval in
 181 outline; a distal and two distolateral zooids budding directly from the ancestrula, the other three
 182 to four periancestrular zooids budding from postancestrular zooids (Figures 3C,E; 4B-C,F; 5B-
 183 C). Zooids are monomorphic and of medium average size. In the zone of early astogeny
 184 autozooids are oval to polygonal in shape, arranged in irregular quincunx. In the zone of
 185 astogenetic repetition, they are larger and longitudinally rectangular, more regular and linearly
 186 arranged, in a brickwall-like alternation pattern between adjacent rows (Figures 3D; 4D-E; 5D).
 187 In the zone of astogenetic repetition, row bifurcations preceded by a wide zooid and followed by
 188 two narrow zooids, one of which is longer than the other (Figures 3D; 4D-E; 5D); occurring
 189 approximately after two to six consecutive zooids. Extensive opesia occupy almost the entire
 190 frontal surface of autozooids. Gymnocyst presumed absent. Cryptocyst narrow, forming a thin
 191 mural rim; normally smooth and worn, with rounded granules rarely preserved (Figure 5D).
 192 Spines bases were not observed and presumed absent. A thin fissure marks zooidal boundaries.
 193 Closure plates not observed. Septula not observed. Kenozooids not observed, presumed absent.
 194
 195 *Remarks.* *Conopeum foliorum* n. sp. resembles the Holocene to Recent type species *Conopeum*
 196 *reticulum* (Linnaeus, 1767) (after López-Gappa and Pereyra, 2020), by having longitudinally
 197 rectangular zooids, by the lack of closure plates, and by having a comparable autozooidal length
 198 (range 0.290 – 0.509, mean 0.392 mm vs range 0.410 – 0.530 mm) and autozooidal width (range
 199 0.129 – 0.271, mean 0.201 vs range 0.210 – 0.320 mm). However, the type species differs by
 200 having a vestigial gymnocyst, cryptocyst strongly developed proximally, and often two triangular
 201 kenozooids present at the proximolateral corners of each autozooid.

202 *Conopeum foliorum* n. sp. resembles the extant *Conopeum seurati* (Canu, 1928), as re-
 203 described by Gordon et al. (2020), in having elongated autozooids, often twice as long as wide,
 204 and a narrow cryptocyst ornamented with rounded granules. However, *C. seurati* differs from *C.*
 205 *foliorum* n. sp. by having larger autozooids (range 0.432 – 0.722 mm, mean 0.574 mm vs mean
 206 0.392 mm), longitudinally sub-rectangular to elongated-oval in shape, cryptocyst surrounded by a
 207 narrow furrow, a slight proximal gymnocyst, up to two distolateral spine bases, and adventitious
 208 kenozooids.

209 *Conopeum flumineum* Taylor and Roger, 2021 from the Upper Cretaceous (upper
 210 Campanian) of the northwestern United States, is closely related to *C. seurati*, and also is similar
 211 to *C. foliorum* n. sp. in having a similar zooid length (range 0.291 – 0.629, mean 0.444 mm vs
 212 mean 0.392), autozooids longitudinally rectangular in outline shape, and in the lack of closure
 213 plates; however, it differs from the new species by its wider autozooids (range 0.291 – 0.629,
 214 mean 0.295 mm vs mean 0.201 mm), with narrow peripheral gymnocyst, cryptocyst surrounded
 215 by a narrow furrow, and the occasionally developed intramural buds. Furthermore, *C. foliorum* n.
 216 sp. shows autozooids normally arranged in well-defined longitudinal rows, in a brickwall-like
 217 alternation pattern between adjacent rows, unlike *C. flumineum*.

218 *Conopeum foliorum* n. sp. resembles *Conopeum okaiana* (Canu, 1911), from the lower
 219 Danian of northern Patagonia, in having no gymnocyst and no pustulose, shelf-like cryptocyst.
 220 However, the Danian species differs from *C. foliorum* n. sp. mainly by its longer (mean 0.476
 221 mm vs mean 0.392 mm) and wider (mean 0.395 mm vs mean 0.201 mm) rounded hexagonal
 222 autozooids with oval or inverted pear-shaped opesia and imperforate closure plates in some
 223 autozooids.

224 ?*Conopeum* sp., from the Upper Cretaceous (upper Campanian) of New Mexico, United
 225 States (Kues, 1983) differs from *C. foliorum* n. sp. by its small distal spine bases and longer
 226 autozooids (~0.55 mm vs mean 0.392 mm). In addition, *Conopeum* sp. from the Upper
 227 Cretaceous (upper Campanian) of southern Utah, United States (Roberts et al., 2008) differs from
 228 *C. foliorum* n. sp. by its substantially longer autozooids (~0.70 mm vs mean 0.392 mm).

229 *Conopeum foliorum* n. sp. also differs from bryozoan specimens identified as
 230 'membraniporimorph' cheilostomes encrusting an angiosperm tree-leaf from the Upper
 231 Cretaceous (Coniacian) in Lower Silesia, Poland (Halamski and Taylor, 2022) by its substantially
 232 longer autozooids (~0.4 mm vs ~0.3 mm).

233 *Conopeum foliorum* n. sp. from the Lefipán Formation differs from other Upper
 234 Cretaceous/Danian *Conopeum* species by normally having longitudinally rectangular-shaped
 235 autozooids (including the extensive opesia of the same shape), and presumably lacking
 236 gymnocyst, pustulose shelf-like cryptocyst, closure plates, and polymorphs. The authors know of
 237 no other comparable species. Although the available material may lack the reliability needed for
 238 discerning some additional fine diagnostic features, *Conopeum foliorum* n. sp. is not conspecific
 239 with any of the known Upper Cretaceous/Danian or younger species referred to *Conopeum*,
 240 supporting the introduction of a new species for this taxon.

241

242 **5. Paleoecology and paleoenvironment**

243
 244 Previous studies have regarded the Paso del Sapo Embayment as an environmental setting
 245 with warm-temperate to warmer conditions and some degree of seasonality. Palynological

246 analyses indicate warm-temperate to subtropical conditions during the deposition of the Lefipán
 247 Formation (Baldoni and Askin, 1993; Nañez and Malumián, 2008). Additionally, the presence of
 248 vegetation adapted to warm and humid conditions, including shore-line mangroves, further
 249 suggests a tropical environment (Barreda et al., 2012). Leaf margin analysis (LMA) and leaf area
 250 analysis (LAA) have estimated an inferred continental mean annual air temperature (MAT) of
 251 approximately 18.5 °C, along with a mean annual precipitation of about 1000 mm (Cúneo et al.,
 252 2021). Evidence of seasonality in the lower Lefipán Formation (Maastrichtian) at the Cañadón
 253 del Loro locality has been inferred from foliar dimorphism of *Araucaria lefipanensis*
 254 (Anduchow-Colombo et al., 2018). Moreover, quantitative estimations indicate a mean annual
 255 sea surface temperature (SST) of around 27 °C for the upper Maastrichtian of the Lefipán
 256 Formation at the San Ramon section, approximately 15 m below the *Turritella* marker bed
 257 (Vellekoop et al., 2017).

258 *Conopeum foliorum* n. sp. is inferred to be from a shallow, likely brackish, environment
 259 within the Lefipán Formation at the San Ramón section. It came from the muddy component of a
 260 horizontally laminated heterolithic bed, associated with coaly plant remains and a few specimens
 261 of euryhaline molluscs (i.e., *Corbicula*, *Ledina*, ?*Nucula*). This sedimentary environment
 262 corresponds to tidal flats (lithofacies H2 of Scasso et al., 2012), supported by the presence of
 263 typical euryhaline bivalves, flat-spiral agglutinated foraminiferans and a high abundance of
 264 peridinioid dinocyst suggesting brackish conditions close to the K/Pg boundary (Nañez and
 265 Malumián, 2008; Vellekoop et al., 2017).

266 The membraniporiform growth habit of *Conopeum foliorum* n. sp. represents one of the most
 267 opportunistic among bryozoan morphotypes, allowing rapid-growth and early reproduction and
 268 colonization of surfaces under suitable conditions (Taylor, 2020; Taylor and Rogers, 2021; and

269 references therein). This growth pattern is common in shallow shelf environments, ranging from
 270 intertidal to upper tidal settings with moderate to high energy levels, where it encrusts hard to
 271 flexible substrates (Bone and Wass, 1990; Nelson et al., 1988; Smith, 1995).

272 Many extant membraniporiform bryozoans, including some comparable *Conopeum* species,
 273 thrive in brackish settings (i.e., lagoons, deltas, estuaries) (Occhipinti Ambrogi, 1985; Poluzzi
 274 and Sabelli, 1985; O'Dea and Okamura, 1999; Taylor, 2020, and references therein). For
 275 example, *Conopeum reticulum* prefers nearshore environments and has been found in estuarine
 276 and euhaline harbours (López-Gappa and Pereyra, 2020), while *Conopeum seurati* exhibits
 277 tolerance to mesohaline to euhaline conditions (14 ‰ to 33 ‰) and even oligohaline (< 5 ‰)
 278 waters (Occhipinti Ambrogi, 1985; O'Dea and Okamura, 1999), categorized recently as
 279 euryhaline (Taylor and Rogers, 2021). These and other brackish water bryozoans typically form
 280 low-diversity communities dominated by non-mineralized ctenostomes and/or cheilostomes with
 281 weakly calcified skeletons (Taylor, 1987, 2005). In addition, some occurrences of brackish water
 282 cheilostome bryozoans have also been identified in the upper Campanian of the Western Interior
 283 Seaway (WIS) in the United States (Kues, 1983; Roberts et al., 2008; Taylor and Rogers, 2021).

284 Upper Cretaceous encrusting cheilostomes demonstrated a versatile ability to colonize
 285 various substrates, including organic and inorganic settlements (Taylor, 2020, and references
 286 therein). They are commonly found cemented to biogenic hard substrates such as mollusc shells
 287 (Aguirre-Urreta and Olivero, 1992; Taylor and McKinney, 2006; Taylor, 2020; Brezina et al.,
 288 2021). In rare cases, bryozoans encrusting dinosaur bones were reported from Upper Cretaceous
 289 rocks of the WIS (Kues, 1983; Taylor and Rogers, 2021). Epiphytic bryozoans have been
 290 documented in the Upper Cretaceous (Maastrichtian) of the Netherlands, associated with fossil
 291 sea-grass (Voigt, 1981). Recently, bryozoans encrusting an angiosperm tree-leaf were found in

292 Upper Cretaceous (Coniacian) rocks of Poland (Halamski and Taylor, 2022). *Conopeum foliorum*
 293 n. sp. utilized remains of both angiosperm and gymnosperm leaves from diverse terrestrial plants
 294 as a substrate (e.g., cf. *Agathis* and several dicot morphotypes).

295 Bryozoans attach to the substrate/host for life, necessitating favourable environmental
 296 conditions for larval settlement and colony growth, including substrate availability, low
 297 sedimentation rates, and sufficient food supply. Given these requirements, the muddy substrate
 298 found at the PLE fossil horizon likely posed challenges to larval settlement for many suspension
 299 feeders, including encrusting bryozoans. Conversely, high sedimentation rates could potentially
 300 impair the filter apparatus, while limited food supply might restrict colony growth. In this regard,
 301 we presumed the required environmental conditions were sufficiently favourable for the
 302 settlement and growth of *Conopeum foliorum* n. sp. Based on sedimentological and
 303 paleoecological data, this setting is interpreted as tidal flats close to vegetated coasts (marsh)
 304 along the margins of tide-dominated delta channels, under significant stress caused by salinity
 305 fluctuations (Scasso et al., 2012). Therefore, *Conopeum foliorum* n. sp. is considered an ancient
 306 opportunistic fast-growing taxon displaying euryhaline habits and preferably colonizing flexible
 307 substrates composed of terrestrial plant leaves deposited in a brackish-water nearshore
 308 environment.

309

310 **6. Concluding remarks**

311

312 We present a new finding regarding a Cretaceous cheilostome bryozoan that encrusts terrestrial
 313 plant leaves, along with a comprehensive taxonomic analysis. We describe and illustrate

314 *Conopeum foliorum* n. sp. discovered in the upper Maastrichtian strata of the Lefipán Formation
315 using contemporary taxonomic methodologies and microscopy techniques. This newly identified
316 taxon in Patagonia likely thrived in a shallow, well-lit, brackish environment influenced by tides,
317 situated within a warm climate at the northwest margin of the Paso del Sapo embayment. Our
318 discoveries also establish *Conopeum foliorum* n. sp. among the earliest known bryozoans from
319 brackish water environments and the second oldest documented instance of bryozoan encrusting
320 terrestrial plant leaves, representing the first such finding in South America.

321

322 **Acknowledgments**

323

324 We thank M. G. Carrera (CONICET) for suggestions that improved the bryozoan taxonomy.
325 Many thanks are expressed to E. Ruigomez (MEF Collection Manager) for his help in the
326 laboratory and for obtaining digital images and extended to L. Canessa (MEF Staff), who
327 prepared the silicon cast. Thanks are also expressed to M. Luque for his help obtaining SEM
328 images at the laboratories of ALUAR S.A. in Puerto Madryn (Chubut). We acknowledge two
329 anonymous reviewers and the handling editor, M. R. Petrizzo, for their very helpful advice and
330 comments that significantly improved this work. Our special thanks to M. Griffin (CONICET)
331 for revision of the English language and improve it. Appreciation is also extended to P. Wilf, K.
332 Johnson, A. Iglesias, and several other MEF and Pennsylvania state students.

333

334 **References**

335

336 Aguirre-Urreta, M.B., Olivero, E.B., 1992. A cretaceous hermit crab from Antarctica: Predatory
 337 activities and bryozoan symbiosis. Antarctic Science 4 (2), 207–214.
 338 <https://doi.org/10.1017/S0954102092000324>

339 Aberhan, M., Kiessling, W., 2014. Rebuilding biodiversity of Patagonian marine molluscs after
 340 the End-Cretaceous Mass Extinction. PLoS ONE 9 (7), e102629.
 341 <https://doi.org/10.1371/journal.pone.0102629>

342 Andruchow-Colombo, A., Escapa, I.H., Cúneo, N.R., Gandolfo, M.A., 2018. *Araucaria*
 343 *lefipanensis* (Araucariaceae), a new species with dimorphic leaves from the Late Cretaceous
 344 of Patagonia, Argentina. American Journal of Botany 105 (6), 1067–1087.
 345 <https://doi.org/10.1002/ajb2.1113>

346 Baldoni, A.M., Askin, R.A., 1993. Palynology of the lower Lefipán Formation (Upper
 347 Cretaceous) of Barranca de los Perros, Chubut province, Argentina. Part II. Angiosperm
 348 pollen and discussion. Palynology 17 (1), 241–264.
 349 <https://doi.org/10.1080/01916122.1993.9989429>

350 Barreda, V.D., Cúneo, N.R., Wilf, P., Currano, E.D., Scasso, R.A., Brinkhuis, H., 2012.
 351 Cretaceous/Paleogene floral turnover in Patagonia: drop in diversity, low extinction, and a
 352 *Classopollis* spike. PLoS ONE 7 (12), 1–8. <https://doi.org/10.1371/journal.pone.0052455>

353 Bone, Y., Wass, R.E., 1990. Sub-Recent bryozoan-serpulid buildups in the Coorong lagoon,
 354 South Australia. Australian Journal of Earth Science 37 (2), 207–214.
 355 <https://doi.org/10.1080/08120099008727921>

356 Brezina, S.S., Taylor, P.D., Romero, M. V., Palópolo, E.E., Casadío, S., 2021. Upper
 357 Maastrichtian and Danian bryozoans from Northern Patagonia, Argentina. *Cretaceous*
 358 *Research*. 125, 104845. <https://doi.org/10.1016/j.cretres.2021.104845>

359 Canu, F., 1911. *Iconographie des Bryozoaires fossiles de l'Argentine. Deuxième Partie. Anales*
 360 *del Museo Nacional de Historia Nattural de Buenos Aires* 14, 215–292.

361 Casamiquela, R.M., 1978. La zona litoral de la transgresión Maastrichtense en el norte de la
 362 Patagonia. *Aspectos ecológicos. Ameghiniana* 15 (1-2), 137–148.

363 Cúneo, R., Andruchow-Colombo, A., De Benedetti, F., Gandolfo, M.A., 2022. D.13. *Megafloras*
 364 de las Formaciones La Colonia y Lefipán, Cretácico Superior de Chubut. In: Giacosa, R.E.
 365 (Ed.), *XXI Congreso Geológico Argentino. Geología y Recursos Naturales de La Provincia*
 366 *Del Chubut. Puerto Madryn*, pp. 261–272.

367 Di Martino, E., Taylor, P.D., 2013. First bryozoan fauna from a tropical Cretaceous carbonate:
 368 *Simsima Formation, United Arab Emirates-Oman border region. Cretaceous Research* 43,
 369 80–96. <https://doi.org/10.1016/j.cretres.2013.02.004>

370 Dick, M.H., Osawa, T., Nodasaka, Y., 2009. Method for making detailed, SEM-suitable VPS
 371 silicone casts of colony molds from fossil bryozoans. *Paleontological Research* 13 (2), 193–
 372 197. <https://doi.org/10.2517/1342-8144-13.2.193>

373 Dick, M.H., Komatsu, T., Takashima, R., Ostrovsky, A.N., 2014. A mid-cretaceous (Albian–
 374 Cenomanian) shell-rubble bryozoan fauna from the Goshoura Group, Kyushu, Japan.
 375 *Journal of Systematic Palaeontology* 12 (4), 401–425.

376 <https://doi.org/10.1080/14772019.2013.765926>

377 Donovan, M.P., Iglesias, A., Wilf, P., Labandeira, C.C., Cúneo, N.R., 2016. Rapid recovery of
 378 Patagonian plant-insect associations after the end-Cretaceous extinction. *Nature Ecology
 379 and Evolution* 1, 0012. <https://doi.org/10.1038/s41559-016-0012>

380 Donovan, M.P., Iglesias, A., Wilf, P., Labandeira, C.C., Cúneo, N.R., 2018. Diverse plant-insect
 381 associations from the latest Cretaceous and early Paleocene of Patagonia, Argentina.
 382 *Ameghiniana* 55 (3), 303–338. <http://dx.doi.org/10.5710/AMGH.15.02.2018.3181>

383 Escapa, I.H., Iglesias, A., Wilf, P., Catalano, S.A., Caraballo-Ortiz, M.A., Cúneo, N.R., 2018.
 384 Agathis trees of Patagonia's Cretaceous-Paleogene death landscapes and their evolutionary
 385 significance. *American Journal of Botany* 105 (8), 1345–1368.
 386 <https://doi.org/10.1002/ajb2.1127>

387 Goin, F.J., Woodburne, M.O., Zimicz, A.N., Martin, G.M., Chornogubsky, L., 2016.
 388 Evolutionary Contexts In: *A Brief History of South American Metatherians*. Springer Earth
 389 System Sciences. Springer, Dordrecht. pp. 125–154. [https://doi.org/10.1007/978-94-017-7420-8_4](https://doi.org/10.1007/978-94-017-

 390 7420-8_4)

391 Gordon, D.P., Sutherland, J.E., Perez, B.A., Waeschenbach, A., Taylor, P.D., Di Martino, E.,
 392 2020. The bryozoan genus *Conopeum* (Electridae) in New Zealand, with description of a
 393 new species and discussion of the morphological and genetic characters of *Conopeum*
 394 *seurati* (Canu, 1928). *Journal of Natural History* 54 (15-16), 947–970.
 395 <https://doi.org/10.1080/00222933.2020.1771452>

396 Håkansson, E., Gordon, D. P., Taylor, P. D., 2024. Bryozoa from the Maastrichtian Korojon
 397 Formation, Western Australia. *Fossils and Strata* 70, 1–155.
 398 <https://doi.org/10.18261/9788215072081-2024>

399 Halamski, A.T., Taylor, P.D., 2022. Angiosperm tree leaf as a bryozoan substrate: a case study
 400 from the Cretaceous and its taphonomic consequences. *Lethaia* 55, 1–7.
 401 <https://doi.org/10.18261/let.55.1.9>

402 Hayward, P., Ryland, J., 1998. Cheilostomatous Bryozoa. Part I. Aeteoidea - Cribrilinoidea:
 403 notes for the identification of British species. In: Barnes, R.S., Crothers, J., (Eds.), *Synopses*
 404 of the British Fauna. Field Studies Council (Shrewsbury), pp. 1–366.

405 Jeffords, R.M., Miller, T.H., 1960. Air brush for whitening fossils, and notes on photography.
 406 *Journal of Paleontology* 34 (2), 275–276.

407 Kelly, S.R., McLachlan, A., 1980. The use of silicon rubbers in the preparation of casts from
 408 natural fossil moulds. *Geological Magazine* 17 (5), 447–454.

409 Kues, B.S., 1983. Bryozoan and crustacean from the Fruitland Formation (Upper Cretaceous) of
 410 New Mexico. *New Mexico Geology* 5 (3), 52–55. <https://doi.org/10.58799/nmg-v5n3.52>

411 López-Gappa, J., Pereyra, C.A., 2020. Bryozoans and borings from Destacamento Río Salado
 412 Member (Buenos Aires Province, Argentina): Systematics and palaeoenvironment. *Journal*
 413 of South American Earth Science

414 102, 102712
<https://doi.org/10.1016/j.jsames.2020.102712>

415 Martha S.O., Taylor P.D., Rader W.L., 2019. Early Cretaceous gymnolaemate bryozoans from

416 the early to middle Albian of the Glen Rose and Walnut formations of Texas, USA. *Journal*
 417 of Paleontology

418 93 (2), 260–277. <https://doi.org/10.1017/jpa.2018.80>

419 Medina, F.A., Olivero, E.B., 1994. Paleontología de la Formación Lefipán (Cretácico-Terciario)
 420 en el valle medio del Río Chubut. *Acta Geológica Lilloana* 48, 104.

421 Nañez, C., Malumián, N., 2008. Paleobiogeografía y paleogeografía del Maastrichtiense marino
 422 de la Patagonia, Tierra del Fuego y la Plataforma Continental Argentina, según sus
 423 foraminíferos bentónicos. *Spanish Journal of Palaeontology* 23 (2), 273–300.

424 Nelson, C.S., Hyden, F.M., Keane, S.L., Leask, W.L., Gordon, D.P., 1988. Application of
 425 Bryozoan zoarial growth-form studies in facies analysis of non-tropical carbonate deposits
 426 in New Zealand. *Sedimentary Geology* 60, 301–322. [https://doi.org/10.1016/0037-0738\(88\)90126-1](https://doi.org/10.1016/0037-0738(88)90126-1)

427 O'Dea, A., Okamura, B., 1999. Influence of seasonal variation in temperature, salinity and food
 428 availability on module size and colony growth of the estuarine bryozoan *Conopeum seurati*.
 429 *Marine Biology* 135, 581–588. <https://doi.org/10.1007/s002270050659>

430 Occhipinti Ambrogi, A., 1985. The zonation of bryozoans along salinity gradients in the Venice
 431 lagoon (northern Adriatic). In: Nielsen, C., Larwood, G.P. (Eds.), *Bryozoa: Ordovician to*
 432 *Recent*. Olsen & Olsen, Viena 1983, pp. 221–232.

433 Olivero, E.B., Medina, F.A., 1994. Sedimentología de la Formación Lefipán (Cretácico-
 434 Terciario) en el valle medio del Río Chubut. *Revista de la Asociación Geológica Argentina*
 435 48, 105–106.

436 Poluzzi, A., Sabelli, B., 1985. Polymorphic zooids in deltaic species populations of *Conopeum*
 437 *seurati* (Canu, 1928) (Bryozoa, Cheilostomata). Delta 6, 265–284.

438 Roberts, E.M., Tapanila, L., Mijal, B., 2008. Taphonomy and sedimentology of storm-generated
 439 continental shell beds: a case example from the Cretaceous Western Interior Basin. The
 440 Journal of Geology 116, 462–479. <https://doi.org/10.1086/590134>

441 Scasso, R.A., Aberhan, M., Ruiz, L., Weidemeyer, S., Medina, F.A., Kiessling, W., 2012.
 442 Integrated bio- and lithofacies analysis of coarse-grained, tide-dominated deltaic
 443 environments across the Cretaceous/Paleogene boundary in Patagonia, Argentina.
 444 Cretaceous Research 36, 37–57. <https://doi.org/10.1016/j.cretres.2012.02.002>

445 Schneider, C. A., Rasband, W. S., Eliceiri, K. W., 2012. NIH Image to ImageJ: 25 years of image
 446 analysis. Nature Methods, 9 (7), 671–675. <https://doi:10.1038/nmeth.2089>

447 Scotese, C.R., 2004. Cenozoic and Mesozoic paleogeography: changing terrestrial biogeographic
 448 pathways. In: Lomolino, M.V., Heaney, L.H., (Eds.), Frontiers of Biogeography new
 449 Directions in the Geography of Nature. Sinauer Associates, Sunderland, MA, pp. 9–26.

450 Smith, A.M., 1995. Palaeoenvironmental interpretation using bryozoans: a review. Geological
 451 Society, London, Special Publications 83 (1), 231–243.
 452 <https://doi.org/10.1144/gsl.sp.1995.083.01.11>

453 Sonar, M.A., Kadu, G.K., Wayal, D. V., 2023. Onychocellidae (Bryozoa) from the Maastrichtian
 454 Kallankurichchi Formation, Ariyalur Group, southern India. Cretaceous Research 144,
 455 105432. <https://doi.org/10.1016/j.cretres.2022.105432>

456 Stiles, E., Wilf, P., Iglesias, A., Gandolfo, M.A., Cúneo, N.R., 2020. Cretaceous-Paleogene
457 plant extinction and recovery in Patagonia. *Paleobiology* 46 (4), 445–469.
458 <https://doi.org/10.1017/pab.2020.45>

459 Taboada, C.A., Pagani, M.A., Cuneo, R., 2018. Primer registro de *Conopeum* Gray, (Electridae,
460 Bryozoa) en el Cretácico Superior de la Formación Lefipán (Chubut, Patagonia). In: Libro
461 de Resúmenes Reunión de Comunicaciones de La Asociación Paleontológica Argentina
462 (RCAPA 2018), Puerto Madryn. Publicación Electrónica de la Asociación Paleontológica
463 Argentina, R80.

464 Taylor, P.D., 1987. Skeletal morphology of malacostegan grade cheilostome Bryozoa. In: Ross,
465 J.R.P., (Ed.), *Bryozoa: Present and Past*. Bellingham: Western Washington University, 269–
466 276.

467 Taylor, P.D., 1995. Late Campanian-Maastrichtian Bryozoa from United Arab Emirates-Oman
468 border. *Bulletin of the Natural History Museum, London (Geology)* 51, 267–273.

469 Taylor, P.D., 2005. Bryozoans and palaeoenvironmental interpretation. *Journal of the*
470 *Palaeontological Society of India* 50 (2), 1–11.

471 Taylor, P.D., 2019. A brief review of the scanty fossil record of Cretaceous bryozoans from
472 Gondwana. *Australasian Palaeontological Memoirs* 52, 147–154.

473 Taylor, P.D., Lazo, D.G., Aguirre-Urreta, M.B., 2009. Lower Cretaceous bryozoans from
474 Argentina: a “by-catch” fauna from the Agrio Formation (Neuquén Basin). *Cretaceous*
475 *Research* 30, 193–203. <https://doi.org/10.1016/j.cretres.2008.07.003>

476 Taylor, P.D., McKinney, F.K., 2006. Cretaceous bryozoa from the Campanian and Maastrichtian
 477 of the Atlantic and Gulf Coastal Plains, United States. *Scripta Geologica* 132, 1–346.

478 Taylor, P.D., Rogers, R.R., 2021. A new cheilostome bryozoan from a dinosaur site in the Upper
 479 Cretaceous (Campanian) Judith River Formation of Montana. *Journal of Paleontology* 95
 480 (5), 965–973. <https://doi.org/10.1017/jpa.2021.34>

481 Vellekoop, J., Holwerda, F., Prámparo, M.B., Willmott, V., Schouten, S., Cúneo, N.R., Scasso,
 482 R.A., Brinkhuis, H., 2017. Climate and sea-level changes across a shallow marine
 483 Cretaceous–Palaeogene boundary succession in Patagonia, Argentina. *Palaeontology* 60 (4),
 484 519–534. <https://doi.org/10.1111/pala.12297>

485 Voigt, E., 1979. The preservation of slightly or non-calcified fossil Bryozoa (Ctenostomata and
 486 Cheilostomata) by bioimmuration. In: Larwood, G., Abbott, M., (Eds.), *Advances in
 487 Byozoology*. Academic Press, London, pp. 541–564.

488 Voigt, E., 1981. Upper Cretaceous bryozoan - seagrass association in the Maastrichtian of the
 489 Netherlands. In: Larwood, G.P., Nielsen, C. (Eds.), *Recent and Fossil Bryozoa*. Olsen &
 490 Olsen, pp. 281–298.

491 Voigt, E., 1983. Preservation of fossils by bioimmuration: *Aetea* (Lamouroux) (bryozoa
 492 cheilostomata) from the mediterranean region (Pliocene and Recent). *Facies* 9, 285–309.

493 Wilf, P., Donovan, M.P., Cúneo, N.R., Gandolfo, M.A., 2017. The fossil flip-leaves
 494 (*Retrophyllum*, Podocarpaceae) of southern South America. *American Journal of Botany*
 495 104, 1344–1369. <https://doi.org/10.3732/ajb.1700158>.

496

497 **Figure captions**

498

499 Figure 1. Location map and stratigraphic section of the K/Pg boundary at San Ramón section,
500 Lefipán Formation. A. Localization of the study area. B. Upper Cretaceous/Paleogene outcrops of
501 Paso del Sapo/Lefipán Formations, including the study area. C. The partial stratigraphic section
502 of the study area corresponds to the upper Maastrichtian/Danian beds of the Lefipán Formation in
503 the San Ramón section. Studied bryozoans were collected from a single fossil-bearing bed
504 indicated as PLE on the figured section ($42^{\circ}40'12''S$, $69^{\circ}49'60''W$). The lower Paleocene (lower
505 Danian) is indicated by the *Turritella* bed (Scasso et al., 2012).

506

507 Figure 2. The northern face of a high cliff shows outcrops of the Lefipán Formation at the San
508 Ramón section, south of the Chubut River.

509

510 Figure 3. Digital camera photographs and scanning electron micrographs of selected specimens
511 of *Conopeum foliorum* n. sp. encrusting a leaf remain of cf. *Agathis* sp. described in Escapa et
512 al., (2018). A. General view of leaf specimen MPEF-PB 8171 overgrowth by numerous bryozoan
513 colonies; (1) MEF-PI 7101-1 (Holotype), (2) MEF-PI 7101-2 (Paratype), (3) MEF-PI 7101-3
514 (Paratype), scale bar = 10 mm. B. SEM detail of the specimens MPEF-PI 7101-1 (Holotype) and
515 MPEF-PI 7101-2 (Paratype) in (A); showing encrusting, multiserial colonies with radial growth
516 pattern, scale bar = 1 mm. C. SEM detail of early astogeny of specimen MPEF-PI 7101-1
517 (Holotype) in (B); showing ancestrula (*) and periancestrular zooids, scale bar = 0.5 mm. D.

518 SEM detail of specimen MPEF-PI 7101-1 (Holotype) in (C); showing elongate rectangular
519 autozooids arranged in a brick-wall pattern and two bifurcated rows, scale bar = 0.1 mm. E. SEM
520 detail of early astogeny of specimen MPEF-PI 7101-2 (Paratype) in (B); showing ancestrula (*)
521 and periancestrular zooids, scale bar = 0.01 mm.

522

523 Figure 4. Digital camera photographs and scanning electron micrographs of selected specimens
524 of *Conopeum foliorum* n. sp. encrusting a dicot leaf remain. A. General view of leaf specimen
525 completely overgrowth by numerous bryozoan colonies; (1) MPEF-PI 7102-1 (Paratype), (2)
526 MPEF-PI 7102-2 (Paratype), (3) MPEF-PI 7102-3 (Paratype), scale bar = 10 mm. B. SEM detail of
527 the specimen MPEF-PI 7102-1 (Paratype) in (A), scale bar = 0.5 mm. C. Detail view of early
528 astogeny of specimen MPEF-PI 7102-1 (Paratype) in (B); showing ancestrula (*) and
529 periancestrular zooids, scale bar = 0.05 mm. D. SEM detail of an autozooid (up left in B), scale
530 bar = 0.1 mm. E. SEM detail of specimen MPEF-PI 7102-1 (Paratype) (down left in B); showing
531 elongate rectangular autozooids arranged in a brick-wall pattern and row bifurcation, scale bar =
532 0.2 mm. F. SEM detail of early astogeny of specimen MPEF-PI 7102-2 (Paratype) in (A);
533 showing ancestrula (*) and periancestrular zooids, scale bar = 0.01 mm.

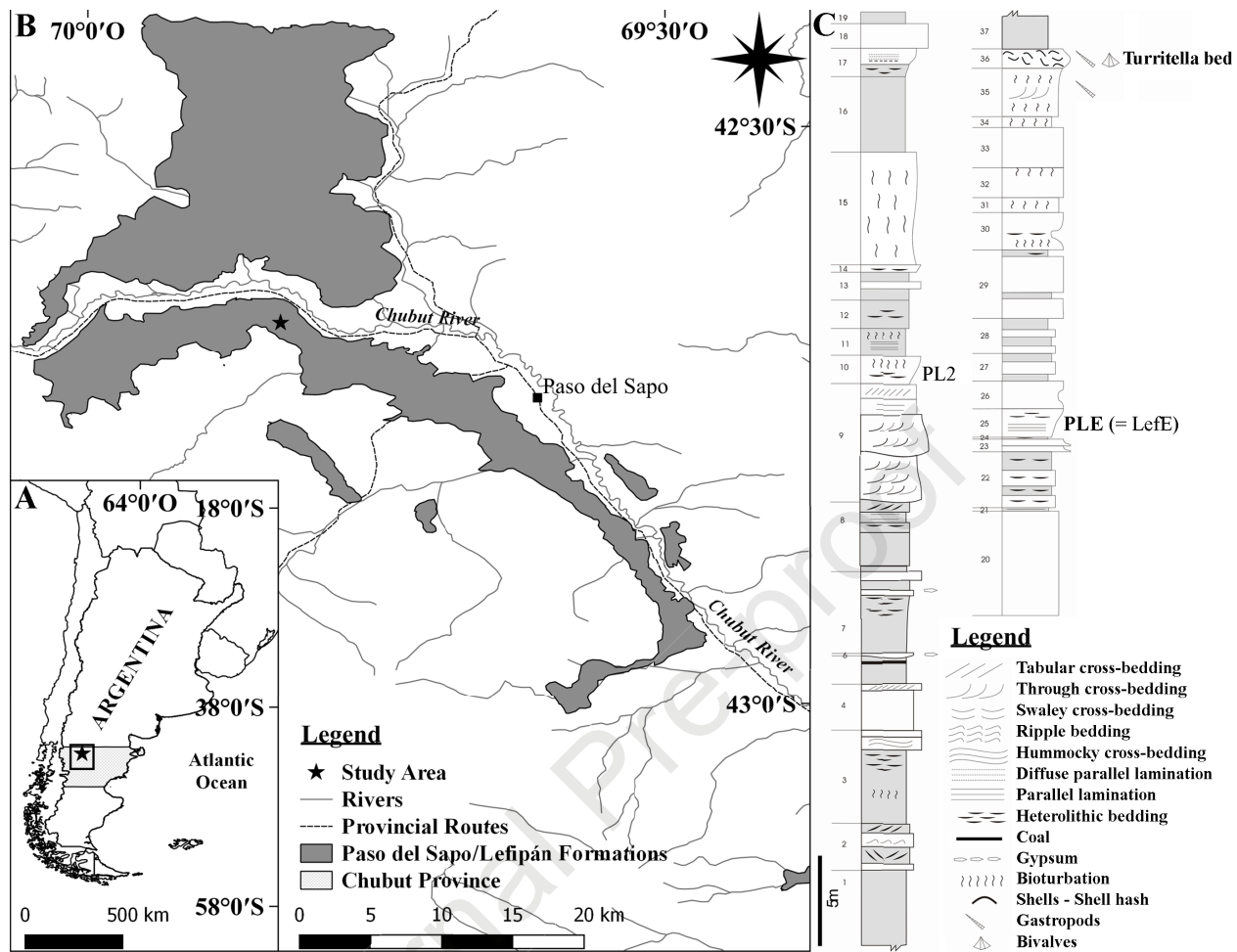
534

535 Figure 5. Digital camera photographs and scanning electron micrographs of selected specimens
536 of *Conopeum foliorum* n. sp. encrusting a dicot leaf remain. A. General view of leaf specimen
537 MPEF-PI 4795 overgrowth by numerous bryozoan colonies; and showing insect-damage (down
538 left), scale bar = 20 mm. B. SEM detail of the specimen MPEF-PI 7106 (Paratype); showing
539 encrusting, multiserial colonies with radial growth pattern, ancestrula (*) and periancestrular
540 zooids, scale bar = 1 mm. C. Detail view of early astogeny of specimen MPEF-PI 7106

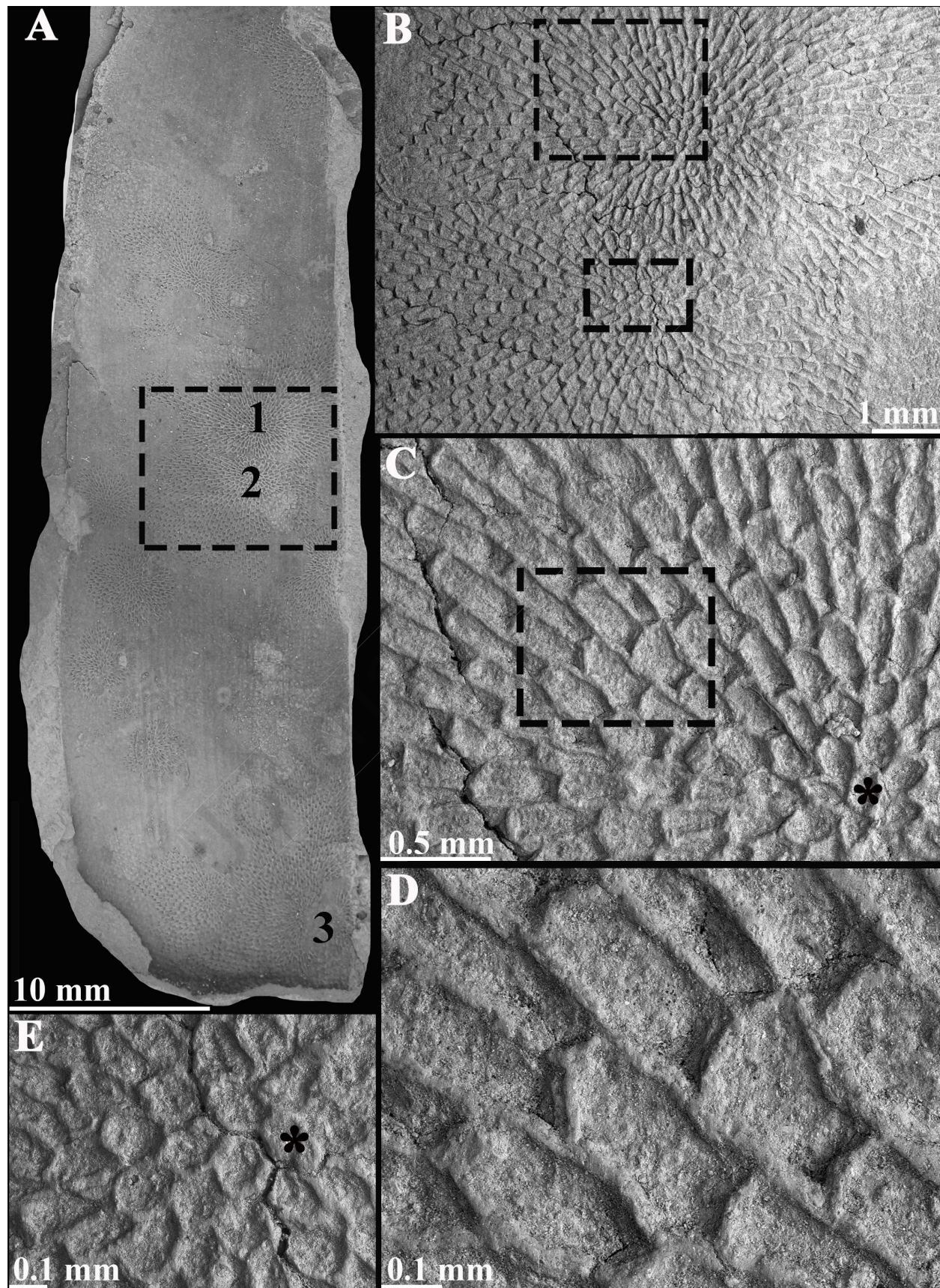
541 (Paratype); showing ancestrula (*) and periancestrular zooids, scale bar = 0.2 mm. D. SEM detail
542 of an autozooid (in B), scale bar = 0.1 mm. E. SEM detail of specimen MPEF-PI 7106 (Paratype)
543 (up left in C); showing elongate rectangular autozooids arranged in a brick-wall pattern and row
544 bifurcation; arrows point to rounded granules, scale bar = 0.2 mm.

Table 1. Measurements of *Conopeum foliorum* n. sp. taken from the type material (i.e. holotype and paratypes; n = 7). Values are expressed in mm; CV in %.

	Mean	SD	CV	MIN	MAX	N
ZL	0.392	0.045	11.426	0.290	0.509	175
ZW	0.201	0.039	19.511	0.129	0.271	175







Journal Pre-proof

